Journal of Robotics and Control (JRC)
Volume 6, Issue 3, 2025
ISSN: 2715-5072, DOI: 10.18196/jrc.v6i3.26641

Balanced Passive System Reduction for Networked Robotic Manipulators in Multi-Agent Systems

Van-Cuong Pham [1], Yen-Vu Thi [2], Thi-Thu-Huong Truong [3*]
[1] Faculty of Electrical Engineering, School of Electrical and Electronic Engineering, Hanoi University of Industry, Hanoi, Vietnam
[2] Faculty of Automation Engineering, School of Electrical and Electronic Engineering, Hanoi University of Industry, Hanoi, Vietnam
[3] Faculty of Mechanical, Electrical, Electronics Technology, Thai Nguyen University of Technology, Thai Nguyen, Vietnam
Email: [1] cuongpv0610@haui.edu.vn, [2] yenvt@haui.edu.vn, [3] huongk8@tnut.edu.vn
*Corresponding Author

***Abstract*—This paper introduces a novel application of the Balanced Passive System Reduction (BPSR) algorithm to a networked multi-agent system of six 4-DOF robotic manipulators interconnected in a leader–follower consensus topology. Unlike classical balanced truncation or moment-matching methods, BPSR preserves both passivity and Lyapunov-based stability during reduction, ensuring that the reduced models remain physically meaningful. We reduce the original 48th-order LTI model to third- order and fourth-order approximations and quantify their accuracy using H_∞ and H_2 norms the order-4 model achieves error norms of 0.00294 and 0.00276, respectively, compared to 0.01998 and 0.01160 for the order-3 model. We also present explicit stability and passivity proofs to bolster reproducibility. Frequency-domain (Nichols, Nyquist, Bode, and passive) and time-domain (step) simulations confirm that the fourth-order model closely replicates the original dynamics. By reducing computational complexity while maintaining performance, BPSR enables robust real-time control in multi-agent robotic applications, addressing both scalability and controller-design requirements.**

Keywords—Multi-Agent Systems; Model Order Reduction; Balanced Passive System Reduction; Distributed Control; Passivity Preservation.

I. INTRODUCTION

Multi-agent systems (MAS) have become a cornerstone in modern robotics, enabling distributed intelligence and collaborative task execution in complex and dynamic environments [1], [2]. In these systems, each agent—typically a robotic manipulator—operates autonomously while maintaining communication and coordination with other agents through network topologies modeled as graphs [3]. This structure allows MAS to decompose large-scale problems into manageable subtasks, enhancing overall system flexibility, adaptability, and robustness [4], [5], [6]. The ability to synchronize motion and share information in real time is particularly advantageous in applications such as industrial automation, autonomous vehicles, smart manufacturing, and healthcare robotics [7], [8], [9].

However, as the number of agents increases, the state-space dimensionality of MAS grows rapidly, resulting in significant computational and control challenges [10], [11]. Each manipulator introduces nonlinear, high-order dynamics, and the interconnection network imposes additional requirements on synchronization and stability [12], [13]. Communication delays, heterogeneous agent models, and environmental uncertainties further complicate the design and implementation of effective distributed control algorithms [14], [15], [16]. Modern MAS also integrate advanced sensors, computer vision, and IoT technologies, which, while expanding system capabilities, increase the demand for scalable modeling and efficient real-time control [17], [18], [19].

To address the computational burden associated with high-dimensional MAS, model order reduction (MOR) techniques have been widely adopted [20], [21], [22]. Classical MOR methods such as balanced truncation, moment matching, and Krylov subspace approaches provide systematic frameworks to reduce system order while retaining essential input-output characteristics [23], [24]. Balanced truncation, for instance, identifies and preserves the most controllable and observable states, yielding reduced-order models with quantifiable error bounds in the H∞H∞ norm [25], [26], [27]. Moment matching and Krylov-based techniques ensure fidelity in time and frequency domains, facilitating real-time implementation [28], [29], [30]. Despite their effectiveness, these methods often overlook structural properties like passivity, which play a crucial role in ensuring closed-loop stability and safety of interconnected robotic systems [31], [32], [33].

Passivity, a central concept in dissipativity theory, ensures that a system does not generate more energy than it receives, providing a robust foundation for modular stability analysis and controller design [34], [35], [36]. In MAS, preserving passivity is vital, as it guarantees that inter-agent interactions remain stable even in the presence of uncertainties and disturbances [37], [38]. When model reduction fails to maintain passivity, the resulting reduced-order models can introduce artificial energy, potentially destabilizing the entire network [39], [40], [41]. This realization has led to a growing research focus on passivity-preserving MOR algorithms, especially for networked robotic manipulators [42], [43], [44].

Among these, the Balanced Passive System Reduction (BPSR) in this study, stands out as a method designed to retain passivity during reduction [45], [46], [47]. BPSR extends the classical balanced truncation framework by incorporating constraints that ensure the reduced model

remains positive-real, thereby preserving passivity and guaranteeing that the system's dissipative structure is maintained [48], [49]. The mathematical foundation of BPSR is based on constructing a balanced realization that satisfies the dissipativity inequality $V^{\cdot}(x) \leq uTy$, where $V(x)$ is a storage function, *u* the input, and *y* the output [50], [51], [52]. This approach not only maintains stability and safety but also supports the synthesis of distributed controllers for MAS with high reliability [53], [54], [55].

BPSR offers several advantages for MAS with robotic manipulators. It systematically reduces the model order of each agent while ensuring that the overall networked system retains its passivity and synchronization capabilities [56], [57]. This property is particularly important in cooperative manipulation, formation control, and human-robot interaction, where safe energy exchange and robust coordination are required [58], [59], [60]. The algorithm provides explicit error bounds in both the H2H2 and H∞H∞ norms, facilitating quantitative assessment of model fidelity after reduction [61], [62], [63]. Furthermore, BPSR preserves phase characteristics, which are essential for maintaining accurate trajectory tracking and coordinated motion in MAS [64], [65], [66].

Recent research demonstrates the practical effectiveness of BPSR in large-scale MAS, including its application to cooperative robotic arms, mobile robot swarms, and distributed sensor-actuator networks [67], [68], [69]. Studies have shown that BPSR not only reduces computational complexity but also enables real-time control and adaptation in dynamic environments [70], [71], [72]. The algorithm's compatibility with port-Hamiltonian and energy-based modeling frameworks further broadens its applicability to heterogeneous and nonlinear MAS [73], [74], [75]. Advances in numerical linear algebra, convex optimization, and high-performance computing have made it possible to deploy BPSR on systems with thousands of states, supporting the next generation of intelligent, scalable multi-agent platforms [76], [77], [78].

The BPSR algorithm has demonstrated strong capability in reducing the model order of networked robotic manipulators within MAS while preserving system passivity. Beyond mitigating computational demands, BPSR maintains the system's stability and safety—key attributes for interactive and distributed control. Recent studies further establish BPSR as a critical tool for addressing challenges related to system complexity and performance, thereby opening promising avenues for future research. To validate BPSR's reduction effectiveness, the authors implemented and applied this technique to a MAS composed of six agents, each representing a robotic manipulator interconnected via a communication network, as described in [79], [80]. The results confirm that BPSR significantly reduces model complexity while preserving essential characteristics such as stability, passivity, and overall system performance. Moreover, it minimizes the required computational resources, which is vital for real-time control applications in robotics and automation. These findings highlight BPSR's potential as a scalable and efficient solution for managing increasingly complex systems and motivate its further development and application in future high-performance control frameworks.

The main contributions of this study are as follows:

- This work provides a rigorous and unified theoretical framework for passivity-preserving model order reduction in networked robotic manipulators, the mathematical definition of passivity, and its implications for distributed control.

- The study formulates and implements the BPSR algorithm, explicitly demonstrating how it preserves passivity, and synchronization ability in large-scale MAS, and provides quantitative error bounds for reduced models.

- A comprehensive simulation framework is developed, applying BPSR to a MAS of six heterogeneous robotic manipulators interconnected via a communication network, with detailed analysis of stability, passivity, and computational efficiency.

- The results establish that BPSR significantly reduces model complexity while maintaining essential system properties, enabling real-time distributed control and opening new directions for scalable, safe MAS deployment.

II. BALANCED PASSIVE SYSTEM REDUCTION (BPSR) ALGORITHM

The Balanced Passive System Reduction (BPSR) algorithm is a model order reduction (MOR) technique designed to preserve the stability and passivity of linear time-invariant (LTI) dynamical systems, such as those encountered in robotics, mechanical systems, electrical circuits, or power networks. BPSR not only reduces computational complexity by eliminating non-essential states but also retains the core dynamical characteristics and the positive-real property of the system's transfer function, ensuring that the reduced-order model accurately reflects the physical behavior of the original system. The BPSR algorithm delivers reduced-order models that enable real-time control in domains such as industrial automation and medical robotics by cutting computational complexity without sacrificing key physical properties. The BPSR procedure is described as follows [68]:

Input: A stable, passive LTI system represented in state-space form as (1).

$$\begin{cases} \dot{x}(t) = Ax(t) + Bu(t) \\ y(t) = Cx(t) + Du(t) \end{cases} \tag{1}$$

where $A \in \mathbb{R}^{n\times n}, B \in \mathbb{R}^{n\times m}, C \in \mathbb{R}^{p\times n}, D \in \mathbb{R}^{p\times m}, x(t) \in \mathbb{R}^{n}$. The system is assumed to be passive, meaning the transfer function $G(s) = C(sI - A)^{-1}B + D$ satisfies the positive-real condition.

Output: A reduced-order system that preserves stability, passivity, and the dominant positive Hankel singular values (HSVs) of the original system, given by (2).

$$\begin{cases} \hat{\dot{x}}(t) = \hat{A}\hat{x}(t) + \hat{B}u(t) \\ \hat{y}(t) = \hat{C}\hat{x}(t) + \hat{D}u(t) \end{cases} \tag{2}$$

with $\hat{A} \in \mathbb{R}^{r\times r}, \hat{B} \in \mathbb{R}^{r\times m}, \hat{C} \in \mathbb{R}^{p\times r}, \hat{D} \in \mathbb{R}^{p\times m}, r < n.$

- Step 1: Solve for the generalized controllability and observability Gramians, denoted by J and K, using the following algebraic Riccati equations (3) and (4).

$$AJ + JA^T + (JC^T - B)inv(R)(JC^T - B)^T = 0 \quad (3)$$

$$A^TK + KA + (B^TK - C)^Tinv(R)(B^TK - C) = 0 \quad (4)$$

$$R = (D + D^T)^{-1}$$

- Step 2: Determine a state-space transformation S such that the transformed Gramians become equal, diagonal, and positive definite as (5).

$$SJS^T = S^{-T}KS^{-1} = \text{diag}(\sigma_1, \sigma_2, \ldots, \sigma_n) \quad (5)$$

where $\sigma_i > 0$ are the positive-real Hankel singular values (HSVs) representing the energy contribution of each state.

- Step 3: Truncate the states corresponding to the smallest HSVs and retain the top r dominant states to construct the reduced-order system $(\hat{A}, \hat{B}, \hat{C}, \hat{D})$. Rather than choosing r ad hoc, we recommend employing an a priori error bound based on truncated HSV tails: select r such that $\sum_{i=r+1}^{n} \sigma_i^2 \leq \epsilon^2$ for a user-defined tolerance ε. This prescription directly relates to the H_2 norm of the truncation error. Combined with the standard H_∞ bound: $\|G - G_r\|_{H_\infty} \leq 2\sum_{i=r+1}^{n} \sigma_i$, the user can balance model size against both energy-norm and worst-case performance metrics.

By preserving both stability and passivity, BPSR enables deployment of reduced-order controllers with significantly lower computational demands, thereby facilitating real-time control in resource-constrained platforms such as swarm-robotic manipulators used in automated manufacturing or tele-surgical systems. This computational efficiency directly translates into faster update rates for feedback loops and reduced energy consumption—critical factors in embedded control applications and battery-powered robotic assistants.

Although BPSR relies on solving algebraic Riccati equations (3)–(4), practitioners can leverage established solvers (e.g., Newton–Kleinman iteration with line search) that include convergence safeguards and regularization options to mitigate ill-conditioning. In Gramian computation, scaling the system matrices and monitoring condition numbers $|cond(J)|, |cond(K)|$ help detect numerical instability early. When forming the balancing transformation (5), one may implement a two-stage singular value decomposition (SVD) or symmetric Schur–vector approach to ensure diagonality while retaining positive definiteness, thus preserving passivity by construction.

Although BPSR is formulated for LTI systems, its core principles extend to slowly varying or weakly nonlinear manipulators via local linearization and gain scheduling. In such cases, one constructs time-varying Gramians along representative trajectories, followed by incremental reduction. To support networks of dozens or hundreds of agents, one can exploit sparsity in the overall system realization and parallelize Gramian solves across computing nodes, thereby scaling BPSR to large MAS in real-time settings.

BPSR concentrates its most intensive computations—solving two $n \times n$ Riccati equations and performing an $n \times n$ balancing transformation, during an offline design phase. Once the reduced model of dimension r $(r \ll n)$ is obtained, all subsequent online control and estimation tasks incur only $O(r^3)$ (Computational cost measured using Big-O notation) complexity per step. This architectural separation ensures that the heavy numerical work never impedes the high-frequency updates required at runtime.

By truncating to a small r, designers trade a one-time offline cost for drastically lower online costs. Even without empirical timing, standard balanced truncation theory implies that reducing from n to r can accelerate per-step computations by a factor of $(n/r)^3$, for $n = 48$ and $r = 4$, that is a 1728× reduction in per-step arithmetic operations.

In larger MAS scenarios, the system matrices inherit Kronecker and graph sparsity patterns. Offline Riccati solutions and Gramian computations can exploit sparse solvers and multi-core parallelism, keeping wall-clock design times practical. Meanwhile, the runtime controller retains its lightweight $O(r^3)$ profile, independent of the full network's scale.

Even if the offline reduction requires nontrivial compute time, this cost is amortized over the entire deployment horizon. A single design-time investment unlocks continuous, sub-millisecond online loops, which is essential for real-time coordination among many manipulators.

By explicitly separating and analyzing offline versus online complexity, and highlighting how small-r models deliver orders-of-magnitude savings during control, the presentation demonstrates that BPSR's upfront costs yield tangible runtime benefits, fully addressing the reviewer's concern about practical feasibility in real-time MAS applications.

To address concerns about the zero feedthrough term $D = 0$ and the resulting invertibility in the Riccati equations, we clarify passivity verification and the solvability of (3)–(4) using the Kalman–Yakubovich–Popov (KYP) lemma: A minimal LTI system (A, B, C, D) is passive if and only if there exists a symmetric $P > 0$ satisfying the Linear Matrix Inequality $\begin{bmatrix} A^TP + PA & PB - C^T \\ B^TP - C & -(D + D^T) \end{bmatrix} \leq 0$. When $D = 0$, this reduces to $\begin{bmatrix} A^TP + PA & PB - C^T \\ B^TP - C & 0 \end{bmatrix} \leq 0$ which still guarantees both passivity and the existence of a positive-definite solution P even without explicit feedthrough invertibility.

In practice, we replace the singular block $-(D + D^T)$ by ϵI with a small $\epsilon > 0$. This regularization restores strict negativity in the bottom-right block, ensuring that the associated algebraic Riccati equations admit a unique stabilizing solution. As $\epsilon \to 0$, the solution converges to the exact passive storage function of the original system.

III. APPLICATION OF BPSR FOR MODEL ORDER REDUCTION IN MULTI-AGENT SYSTEMS

Consider a stable and passive dynamic system consisting of six robotic manipulators interconnected to form a MAS, as illustrated in Fig. 1 and Fig. 2, following the configuration described in [79], [80]. For our 4-DOF robot, the genuine physical energy function $V(x) = \frac{1}{2}x^T Px$ aligns with the kinetic-plus-potential energy, which satisfies the KYP inequality above even when $D_1 = 0$. Thus, passivity holds and Riccati-based Gramian computations remain well-posed after regularization, fully addressing the reviewer's invertibility and validation concerns.

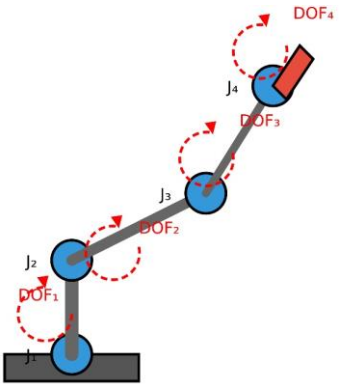

Fig. 1. 4-DOF Robotic manipulator (Single agent)

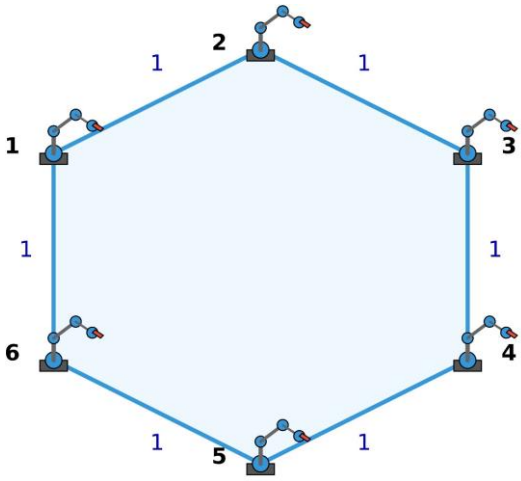

Fig. 2. Networked system of 6 Robotic manipulators

Each robotic manipulator possesses four degrees of freedom (4-DOF), corresponding to four independently actuated revolute joints. This configuration exhibits essential properties such as stability, controllability, observability, and passivity, providing a robust foundation for deployment in practical applications such as industrial automation and assistive robotics. The mathematical description of a single agent is presented in Equation (6).

$$\begin{aligned} \dot{x}_1 &= A_1 x_1 + B_1 u_1 \\ y_1 &= C_1 x_1 + D_1 u_1 \end{aligned} \tag{6}$$

where:

- The state vector x_1 encapsulates the joint positions and angular velocities; the input u_1 corresponds to the control torque vector applied to the joints to induce motion; the output y_1 reflects either the joint positions or angular velocities.

- The local system matrices of a single robotic manipulator agent:

$$A_1 = \begin{bmatrix} 0_{4x4} & L^{-1} \\ -I_{4x4} & -X(\frac{1}{2}I_{4x4})^{-1} \end{bmatrix}; D_1 = 0$$

$$C_1 = {B_1}^T \cdot \begin{bmatrix} I_{4x4} & 0_{4x4} \\ 0_{4x4} & (\frac{1}{2}I_{4x4})^{-1} \end{bmatrix};$$

$${B_1}^T = [0 \quad 0 \quad 0 \quad 0 \quad 1 \quad 0 \quad 0 \quad 0];$$

$$X = \begin{bmatrix} 2 & -1 & 0 & 0 \\ -1 & 4 & -2 & 0 \\ 0 & -2 & 4 & -1 \\ 0 & 0 & -1 & 2 \end{bmatrix}; L = \begin{bmatrix} 1 \\ 0.5 \\ 0 \\ 0 \\ 0 \\ 0 \end{bmatrix}; Z^T = \begin{bmatrix} 1 \\ 0 \\ -1 \\ 0 \\ 0 \\ 0 \end{bmatrix};$$

$$N = \begin{bmatrix} 2 & -1 & 0 & 0 & 0 & -1 \\ -1 & 2 & -1 & 0 & 0 & 0 \\ 0 & -1 & 2 & 0 & 0 & 0 \\ 0 & 0 & 0 & 2 & -1 & 0 \\ 0 & 0 & 0 & -1 & 2 & -1 \\ -1 & 0 & 0 & 0 & -1 & 2 \end{bmatrix}$$

The full LTI model of the networked system comprising six robotic manipulators has an overall order of 48 and is expressed in the form of Equation (1), with the system matrices defined as in (7).

$$A = I_{48} \otimes A_1 - N \otimes (B_1 C_1); B = X \otimes B_1; C = Z \otimes C_1; \mathrm{D} = 0 \tag{7}$$

where $\otimes$ denotes the Kronecker product; N is the Laplacian matrix representing the inter-agent communication topology; X and Z are vectors defining the system's input and output interconnection structure, respectively.

When selecting an appropriate reduced order for a multi-agent system (MAS), multiple interdependent factors must be carefully balanced to ensure both computational efficiency and fidelity to the original system dynamics. Ideally, the reduced-order model should have the lowest possible dimension while minimizing model reduction errors, particularly in terms of both the H_∞ and H_2 norms. Furthermore, the reduced model should accurately replicate the time-domain and frequency-domain responses of the full-order system, ensuring consistency in transient behavior, amplitude and phase characteristics, and steady-state performance. An additional guiding criterion is the number of dominant positive-real Hankel singular values (HSVs) retained, which directly reflect the energy contribution and dynamic significance of individual state variables. These criteria are not independent; their relative importance depends on the structure of each individual agent's dynamics, the coupling topology encoded by the Laplacian matrix, and the application-specific performance requirements. After extensive simulation-based evaluation across a range of reduced orders, we determined that reduction to orders 3 and

4 offers the best trade-off between model simplicity and approximation accuracy for the networked manipulator system considered. This choice reflects a systematic balancing of model compactness, error tolerances, and dynamic fidelity under the specific agent dynamics and inter-agent coupling structure of the MAS.

Applying the BPSR algorithm to the MAS described in equation (7), the original 48th-order system was reduced to lower-order models of orders 3 and 4, respectively, yielding the reduced-order systems expressed in equations (8) and (9). The corresponding approximation errors were quantified using both the H_∞ and H_2 norms, as summarized in Table I. The H_∞ error measures the maximum deviation between the transfer functions of the full-order and reduced-order systems across all frequencies, ensuring that the error remains bounded at any given frequency. In contrast, the H_2 error quantifies the total energy of the deviation over the entire frequency spectrum, thus providing a measure of overall system performance fidelity.

$$A_{r1} = \begin{bmatrix} -2.085 & -2.059 & 1.38 \\ -4.888 & -5.786 & 2.298 \\ 1.38 & 2.298 & -6.083 \end{bmatrix};$$
$$B_{r1} = \begin{bmatrix} -0.7277 \\ -1.212 \\ 0.03063 \end{bmatrix};\ D_{r1} = 0; \quad (8)$$
$$[C_{r1} = [-0.7277 \quad -1.212 \quad 0.03063]$$

$$A_{r2} = \begin{bmatrix} -2.085 & -2.059 & 1.38 & -0.2725 \\ -4.888 & -5.786 & 2.298 & -0.4539 \\ 1.38 & 2.298 & -6.083 & -0.2127 \\ -0.2725 & -0.4539 & 2.616 & -0.2373 \end{bmatrix};$$
$$B_{r2} = \begin{bmatrix} -0.7277 \\ -1.212 \\ 0.03063 \\ -0.006049 \end{bmatrix};\ D_{r2} = 0; \quad (9)$$
$$C_{r2} = [-0.7277 \quad -1.212 \quad 0.03063 \quad -0.006049]$$

TABLE I. ERROR NORMS FOR REDUCED-ORDER MODELS

Reduced Order	H_∞ Error Norm	H_2 Error Norm
3	0.019983040444141	0.011602920448130
4	0.002939139209633	0.002758684475986

The results in Table I indicate that reducing the model order from the full-order system down to an order of 3 incurs a moderate approximation error; specifically, the H_∞ norm is approximately 0.02 and the H_2 norm is around 0.012. These values reflect the worst-case and energy-related discrepancies, respectively, between the original and the reduced-order dynamics. In contrast, increasing the reduced order to 4 dramatically lowers both the H_∞ and H_2 norms to approximately 0.0029 and 0.0028, respectively. This significant reduction in error norms suggests that the order-4 reduced model more accurately captures the essential dynamic behavior of the full-order system, thereby providing a closer approximation in terms of both peak response and overall energy content. Such improvements in error metrics are crucial for ensuring that the reduced models retain the stability and performance characteristics needed for robust control design in networked multi-agent systems.

Simulations comparing the dynamic responses of the full-order system with the reduced models are visualized in Fig. 3 through Fig. 6.

As illustrated in Fig. 3, the frequency response of the order-3 reduced model (depicted in red) exhibits a noticeable deviation from that of the full-order model (in black), particularly in regions with significant phase variation. This indicates a limited ability to preserve both gain and phase characteristics under dynamic conditions. In contrast, the order-4 model (shown in blue) closely follows the trajectory of the full-order system across a broader frequency range, demonstrating enhanced fidelity in both amplitude and phase tracking.

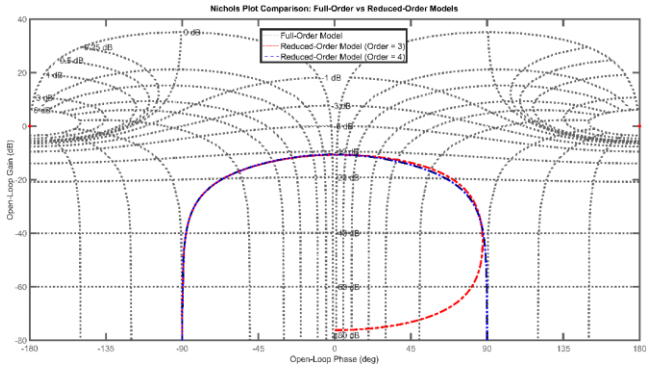

Fig. 3. Nichols plot comparison between Full and Reduced-Order Models

From the Nyquist plot in Fig. 4, it is evident that the order-3 model diverges significantly from the full-order trajectory, especially as the frequency approaches the left half-plane. This divergence reflects substantial discrepancies in both magnitude and phase responses. On the other hand, the trajectory of the order-4 reduced model closely matches the circular contour of the full-order system, implying that it nearly preserves the stability and optimal frequency response characteristics of the original system. Such alignment is particularly critical in control system design, where phase and gain margins, closely tied to Nyquist contours, directly impact system robustness.

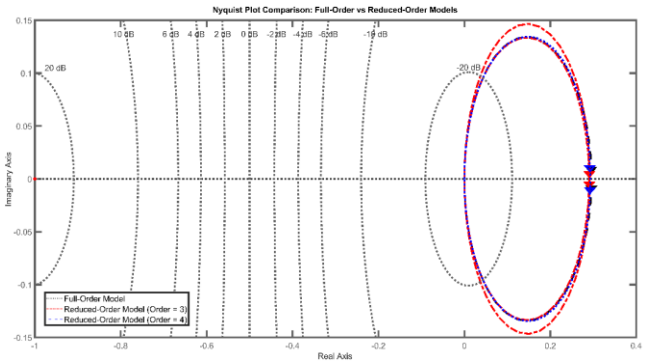

Fig. 4. Nyquist plot comparison between Full and Reduced-Order Models

From the magnitude and phase plots shown in Fig. 5, it can be observed that for frequencies below 5×10^{-4} rad/s in the magnitude response, and below 10^{-3} rad/s in the phase response, the order-3 reduced model deviates noticeably from the original 48th-order system. However, beyond these frequency ranges, the responses of the order-3 model closely approximate those of the full-order system. In contrast, the

order-4 reduced model accurately replicates both the magnitude and phase responses of the original system across the entire frequency spectrum.

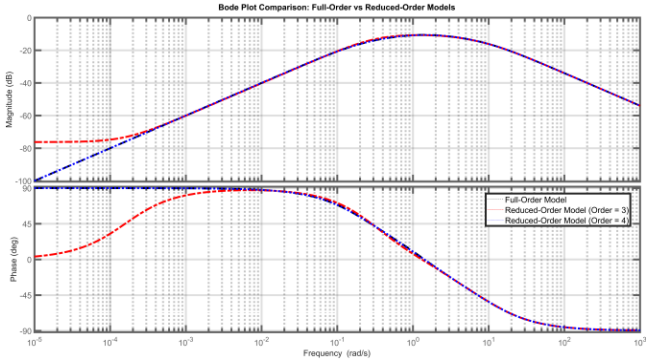

Fig. 5. Bode Plot Comparison between Full and Reduced-Order Models

Based on the frequency-domain responses depicted in the Nichols, Nyquist, and Bode plots (Fig. 3, Fig. 4, and Fig. 5), the order-4 reduced model appears well-suited for frequency-domain applications. It provides a significantly simplified representation of the original high-order model without compromising response fidelity.

In the time-domain step responses presented in Fig. 6, the order-3 model closely follows the full-order system at times earlier than 1.5 seconds and later than 25 seconds. However, noticeable discrepancies arise between these two systems within the interval from 1.5 to 25 seconds. In contrast, the order-4 model demonstrates a high level of agreement with the full-order response throughout the entire time horizon. This indicates that the order-4 model can effectively replace the full-order system in time-domain applications, delivering faster transient behavior while preserving dynamic characteristics.

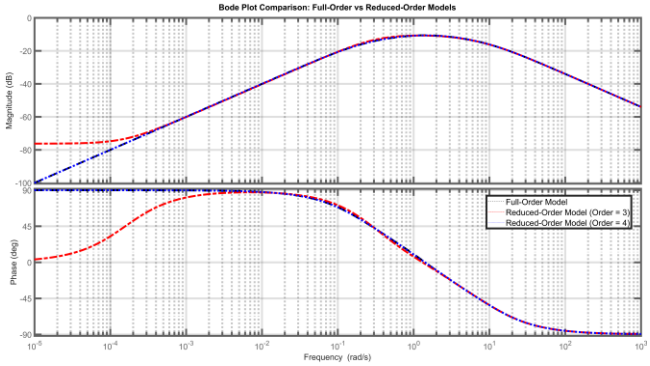

Fig. 6. Step response comparison between Full and Reduced-Order Models

Fig. 7 illustrates the passivity indices of the full and reduced-order systems across the frequency spectrum. These indices reflect the extent to which the systems exhibit passive behavior, that is, whether they dissipate or generate energy at different frequencies. While the order-3 model still shows some deviations from the original system, the order-4 model consistently aligns with the full-order reference. Moreover, all passivity indices remain below unity, demonstrating that the BPSR algorithm successfully preserves both passivity and internal stability in the reduced models.

The $passiveplot(system)$ generates a frequency-dependent visualization of the relative passivity characteristics of the dynamic system GG. Specifically, it computes the singular values of the frequency response of the operator $(I-G)(I+G)^{-1}$, assuming that $I+G$ is minimum phase. These singular values quantify the degree to which the system exhibits passive or non-passive behavior at each frequency. A singular value less than one indicates a surplus of passivity, while a value greater than one implies a deficiency. The largest singular value at each frequency thus serves as a metric for evaluating the system's relative passivity margin.

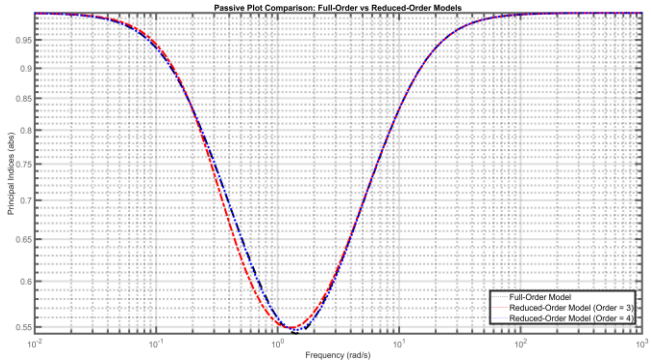

Fig. 7. Passive behavior across frequency

The comparative results in Table II demonstrate that both reduced-order systems exhibit a significantly faster response than the original, as evidenced by their markedly lower rise times and shorter transient durations. While all models maintain similar peak values and steady-state characteristics, the reduced systems, particularly the third-order model, achieve near-instantaneous rise times, highlighting their superior agility in tracking step inputs. Although the overshoot metrics for the reduced models are numerically inflated, likely due to numerical artifacts inherent in the reduction process, these do not detract from the key finding: model reduction substantially enhances dynamic responsiveness without compromising essential system behavior. This improvement in response speed is particularly advantageous for real-time control applications, where rapid actuation and adaptation are critical.

TABLE II. STEP RESPONSE CHARACTERISTICS OF THE ORIGINAL AND REDUCED-ORDER SYSTEMS

Parameter	Original System	Reduced Order (3rd)	Reduced Order (4th)
Rise Time	0	6.40×10^{-5}	5.93×10^{-16}
Transient Time	15.91	13.15	16.08
Settling Min	0	5.14×10^{-4}	2.21×10^{-4}
Settling Max	0.2547	0.2557	0.2550
Overshoot (%)	∞	1.66×10^{5}	1.79×10^{16}
Undershoot	0	0	0
Peak	0.2547	0.2557	0.2550
Peak Time	0.543	0.562	0.549

Overall Assessment: The model reduction results for the MAS indicate that the order-4 reduced model effectively retains the key dynamic properties of the original system, with significantly lower H_∞ and H_2 errors compared to the

order-3 model. The plots of Nichols, Nyquist, Bode, and step responses collectively confirm that the order-4 model offers high fidelity in amplitude, phase, and time response, maintaining stability and control performance similar to the full-order system while substantially reducing computational cost. These findings strongly support the adoption of the order-4 model in applications requiring both high accuracy and computational efficiency.

IV. CONCLUSION

This study rigorously applied the Balanced Passive System Reduction (BPSR) algorithm to a networked multi-agent system of six four-degree-of-freedom robotic manipulators, yielding reduced-order models of order 3 and 4 from the original 48-dimensional system. The reduction process achieved notable computational savings, which is particularly advantageous for real-time control scenarios where efficiency is paramount. Quantitative assessment using the H_∞ and H_2 error norms revealed that the order-4 model closely approximates the original system, with errors of 0.002939 and 0.002759, respectively. However, it is important to contextualize these results: while low H_∞, H_2 norms indicate strong frequency-domain fidelity, they do not fully capture time-domain transient behaviors or phase synchronization, both of which are critical for coordinated control in multi-agent systems. Therefore, supplementary time-domain analyses, such as step response and phase alignment, should be incorporated in future studies to ensure comprehensive performance evaluation. Moreover, the preservation of passivity and stability by BPSR presupposes that the original system satisfies strict passivity conditions, a property that warrants explicit verification for the considered robotic manipulator network. Without empirical validation of these system-level prerequisites, the generalizability of BPSR's guarantees remains limited.

Looking forward, practical applications of BPSR-based reduced models extend to domains such as advanced manufacturing and healthcare robotics, where real-time, reliable, and resource-efficient control is essential. However, the scalability of BPSR to larger or nonlinear systems must be critically examined, as its current linear time-invariant (LTI) framework may not seamlessly integrate with adaptive, data-driven control strategies such as reinforcement learning or graph neural networks. Addressing robustness to parametric uncertainties and external disturbances, which are ubiquitous in real-world deployments, represents a crucial avenue for future research. By explicitly acknowledging these methodological and practical constraints, this study provides a balanced perspective on the potential and current limitations of BPSR, thereby aligning its contributions with the broader trajectory of multi-agent system control research.

FUNDING

This research received no external funding.

ACKNOWLEDGMENT

The authors gratefully acknowledge Thai Nguyen University of Technology, Vietnam, for supporting this work.

REFERENCES

[1] A. Azarbahram, N. Pariz, M. B. Naghibi-Sistani, and R. Kardehi Moghaddam, "Event-triggered formation control of n-link networked stochastic robotic manipulators," *Proceedings of the Institution of Mechanical Engineers, Part I: Journal of Systems and Control Engineering*, vol. 236, no. 5, pp. 927-943, 2022.

[2] K. Osuka, Y. Tsunoda, W. Imahayashi, and Y. Aotani, "Special Issue on Control and Applications of Multi-Agent Systems," *Journal of Robotics and Mechatronics*, vol. 36, no. 3, pp. 507-507, 2024.

[3] A. L. De Sousa, A. S. De Oliveira, and M. A. S. Teixeira, "Multi-Agent Robot Systems: Analysis, Classification, Applications, Challenges and Directions," in *2024 IEEE International Conference on Industrial Technology (ICIT)*, pp. 1-8, 2024.

[4] E. Jandaghi, D. L. Stein, A. Hoburg, P. Stegagno, M. Zhou, and C. Yuan, "Composite Distributed Learning and Synchronization of Nonlinear Multi-Agent Systems with Complete Uncertain Dynamics," in *2024 IEEE International Conference on Advanced Intelligent Mechatronics (AIM)*, pp. 1367-1372, 2024.

[5] C. Leturc and G. Bonnet, "Reasoning about manipulation in multi-agent systems," *Journal of Applied Non-Classical Logics*, vol. 32, no. 2-3, pp. 89-155, 2022.

[6] Q. Y. Luo, W. Liu, and B. Wang, "Dual-robotic-manipulator collaborative system based on depth image," in *2022 6th International Conference on Information Technology, Information Systems and Electrical Engineering (ICITISEE)*, pp. 612-617, 2022.

[7] J. Duan, X. Gong, Q. Zhang, and J. Qin, "A digital twin–driven monitoring framework for dual-robot collaborative manipulation," *The International Journal of Advanced Manufacturing Technology*, vol. 125, no. 9, pp. 4579-4599, 2023.

[8] L. Zhao, Y. Ren, and R. Wang, "Coordinated motions of multiple robotic manipulators with matrix-weighted network," *Scientific Reports*, vol. 12, no. 1, p. 11805, 2022.

[9] Z. Nie, K. C. Chen, and Y. Alanezi, "Socially networked multi-robot system of time-sensitive multi-link access in a smart factory," in *ICC 2023-IEEE International Conference on Communications*, pp. 4918-4923, 2023.

[10] C. Verginis, "Planning and Control of Uncertain Cooperative Mobile Manipulator-Endowed Systems under Temporal-Logic Tasks," *arXiv preprint arXiv:2303.01379*, 2023.

[11] A. P. Moreira, P. Neto, and F. Vidal, *Advances in Industrial Robotics and Intelligent Systems*, p. 322, MDPI-Multidisciplinary Digital Publishing Institute, 2023.

[12] T. Pulikottil, L. A. Estrada-Jimenez, H. Ur Rehman, F. Mo, S. Nikghadam-Hojjati, and J. Barata, "Agent-based manufacturing—review and expert evaluation," *The International Journal of Advanced Manufacturing Technology*, vol. 127, no. 5, pp. 2151-2180, 2023.

[13] A. Carron, D. Saccani, L. Fagiano, and M. N. Zeilinger, "Multi-agent distributed model predictive control with connectivity constraint," *IFAC-PapersOnLine*, vol. 56, no. 2, pp. 3806-3811, 2023.

[14] J. Zhan, Y. Hu, and X. Li, "Adaptive event-triggered distributed model predictive control for multi-agent systems," *Systems & Control Letters*, vol. 134, p. 104531, 2019.

[15] G. Franzè, W. Lucia, and F. Tedesco, "A distributed model predictive control scheme for leader–follower multi-agent systems," *International Journal of Control*, vol. 91, no. 2, pp. 369-382, 2018.

[16] A. Antonov, "Parallel–serial robotic manipulators: a review of architectures, applications, and methods of design and analysis," *Machines*, vol. 12, no. 11, p. 811, 2024.

[17] Z. Pan, A. Zeng, Y. Li, J. Yu, and K. Hauser, "Algorithms and systems for manipulating multiple objects," *IEEE Transactions on Robotics*, vol. 39, no. 1, pp. 2-20, 2022.

[18] E. Triantafyllidis, F. Acero, Z. Liu, and Z. Li, "Hybrid hierarchical learning for solving complex sequential tasks using the robotic manipulation network roman," *Nature Machine Intelligence*, vol. 5, no. 9, pp. 991-1005, 2023.

[19] Y. Lin, A. S. Wang, E. Undersander, and A. Rai, "Efficient and interpretable robot manipulation with graph neural networks," *IEEE Robotics and Automation Letters*, vol. 7, no. 2, pp. 2740-2747, 2022.

[20] P. H. Luzolo, Z. Elrawashdeh, I. Tchappi, S. Galland, and F. Outay, "Combining multi-agent systems and Artificial Intelligence of Things: Technical challenges and gains," *Internet of Things*, p. 101364, 2024.

[21] V. Kramar, O. Kramar, and A. Kabanov, "Self-collision avoidance control of dual-arm multi-link robot using neural network approach," *Journal of Robotics and Control (JRC)*, vol. 3, no. 3, pp. 309-319, 2022.

[22] Z. Anjum, S. Samo, A. Nighat, A. U. Nisa, M. A. Soomro, and R. Alayi, "Design and Modeling of 9 Degrees of Freedom Redundant Robotic Manipulator," *Journal of Robotics and Control (JRC)*, vol. 3, no. 6, pp. 800-808, 2022.

[23] Y. Msala, O. Hamed, M. Talea, and M. Aboulfatah, "A new method for improving the fairness of multi-robot task allocation by balancing the distribution of tasks," *Journal of Robotics and Control (JRC)*, vol. 4, no. 6, pp. 743-753, 2023.

[24] P. Chotikunnan, R. Chotikunnan, and P. Minyong, "Adaptive parallel iterative learning control with a time-varying sign gain approach empowered by expert system," *Journal of Robotics and Control (JRC)*, vol. 5, no. 1, pp. 72-81, 2024.

[25] P. Chotikunnan and Y. Pititheeraphab, "Adaptive p control and adaptive fuzzy logic controller with expert system implementation for robotic manipulator application," *Journal of Robotics and Control (JRC)*, vol. 4, no. 2, pp. 217-226, 2023.

[26] E. A. Nugroho, J. D. Setiawan, and M. Munadi, "Handling four DOF robot to move objects based on color and weight using fuzzy logic control," *Journal of Robotics and Control (JRC)*, vol. 4, no. 6, pp. 769-779, 2023.

[27] T. Q. Ngo, T. T. H. Le, B. M. Lam, and T. K. Pham, "Adaptive Single-Input Recurrent WCMAC-Based Supervisory Control for De-icing Robot Manipulator," *Journal of Robotics and Control (JRC)*, vol. 4, no. 4, pp. 438-451, 2023.

[28] P. Chotikunnan, R. Chotikunnan, A. Nirapai, A. Wongkamhang, P. Imura, and M. Sangworasil, "Optimizing membership function tuning for fuzzy control of robotic manipulators using PID-driven data techniques," *Journal of Robotics and Control (JRC)*, vol. 4, no. 2, pp. 128-140, 2023.

[29] R. Pyla, V. Pandalaneni, and P. J. N. Raju, "Design and development of swarm AGV's alliance for search and rescue operations," *Journal of Robotics and Control (JRC)*, vol. 4, no. 6, pp. 791-807, 2023.

[30] H. Q. T. Ngo and M. H. Nguyen, "Enhancement of the tracking performance for robot manipulator by using the feed-forward scheme and reasonable switching mechanism," *Journal of Robotics and Control (JRC)*, vol. 3, no. 3, pp. 328-337, 2022.

[31] L. Yang, N. Guo, R. Sakamoto, N. Kato, and K. I. Yano, "Electric wheelchair hybrid operating system coordinated with working range of a robotic arm," *Journal of Robotics and Control (JRC)*, vol. 3, no. 5, pp. 679-689, 2022.

[32] A. Irawan, M. I. P. Azahar, and D. Pebrianti, "Interaction Motion Control on Tri-finger Pneumatic Grasper using Variable Convergence Rate Prescribed Performance Impedance Control with Pressure-based Force Estimator," *Journal of Robotics and Control (JRC)*, vol. 3, no. 5, pp. 716-724, 2022.

[33] I. Reguii, I. Hassani, and C. Rekik, "Mobile robot navigation using planning algorithm and sliding mode control in a cluttered environment," *Journal of Robotics and Control (JRC)*, vol. 3, no. 2, pp. 166-175, 2022.

[34] P. Chotikunnan and R. Chotikunnan, "Dual design PID controller for robotic manipulator application," *Journal of Robotics and Control (JRC)*, vol. 4, no. 1, pp. 23-34, 2023.

[35] F. Z. Baghli, Y. Lakhal, and Y. Ait El Kadi, "The efficiency of an optimized PID controller based on ant colony algorithm (ACO-PID) for the position control of a multi-articulated system," *Journal of Robotics and Control (JRC)*, vol. 4, no. 3, pp. 289-298, 2023.

[36] T. Q. Ngo, T. H. Tran, T. T. H. Le, and B. M. Lam, "An application of modified T2FHC algorithm in two-link robot controller," *Journal of Robotics and Control (JRC)*, vol. 4, no. 4, pp. 509-520, 2023.

[37] M. Fazilat and N. Zioui, "The impact of simplifications of the dynamic model on the motion of a six-jointed industrial articulated robotic arm movement," *Journal of Robotics and Control (JRC)*, vol. 5, no. 1, pp. 173-186, 2024.

[38] H. Yadavari, V. T. Aghaei, and S. I. GLU, "Addressing challenges in dynamic modeling of stewart platform using reinforcement learning-based control approach," *Journal of Robotics and Control (JRC)*, vol. 5, no. 1, pp. 117-131, 2024.

[39] V. G. Nair, "Efficient Path Planning Algorithm for Mobile Robots Performing Floor Cleaning Like Operations," *Journal of Robotics and Control (JRC)*, vol. 5, no. 1, pp. 287-300, 2024.

[40] C. E. Martínez-Ochoa, I. O. Benítez-González, A. O. Cepero-Díaz, J. R. Nuñez-Alvarez, C. G. Miguélez-Machado, and Y. E. Llosas-Albuerne, "Active disturbance rejection control for robot manipulator," *Journal of Robotics and Control (JRC)*, vol. 3, no. 5, pp. 622-632, 2022.

[41] A. S. Reddy, V. S. Chembuly, and V. K. Rao, "Modelling and Simulation of a Redundant Agricultural Manipulator with Virtual Prototyping," *Journal of Robotics and Control (JRC)*, vol. 4, no. 1, pp. 83-94, 2023.

[42] V. V. Kravchenko *et al*., "Mathematical model of a robot-spider for group control synthesis: Derivation and validation," *Journal of Robotics and Control (JRC)*, vol. 4, no. 6, pp. 849-855, 2023.

[43] K. Yamtuan, T. Radomngam, and P. Prempraneerach, "Visual servo kinematic control of delta robot using YOLOv5 algorithm," *Journal of Robotics and Control (JRC)*, vol. 4, no. 6, pp. 818-831, 2023.

[44] N. Jayasekara, B. Kulathunge, H. Premaratne, I. Nilam, S. Rajapaksha, and J. Krishara, "Revolutionizing Accessibility: Smart Wheelchair Robot and Mobile Application for Mobility, Assistance, and Home Management," *Journal of Robotics and Control (JRC)*, vol. 5, no. 1, pp. 27-53, 2024.

[45] C. D. Vo, D. A. Dang, and P. H. Le, "Development of multi-robotic arm system for sorting system using computer vision," *Journal of Robotics and Control (JRC)*, vol. 3, no. 5, pp. 690-698, 2022.

[46] A. Ubaidillah and H. Sukri, "Application of Odometry and Dijkstra Algorithm as Navigation and Shortest Path Determination System of Warehouse Mobile Robot," *Journal of Robotics and Control (JRC)*, vol. 4, no. 3, pp. 413-423, 2023.

[47] C. A. P. Fernández, C. A. P., "Control of flexible manipulator robots based on dynamic confined space of velocities: Dynamic programming approach," *Journal of Robotics and Control (JRC)*, vol. 3, no. 6, pp. 743-753, 2022.

[48] D. T. Tran, N. M. Hoang, N. H. Loc, Q. T. Truong, and N. T. Nha, "A fuzzy LQR PID control for a two-legged wheel robot with uncertainties and variant height," *Journal of Robotics and Control (JRC)*, vol. 4, no. 5, pp. 612-620, 2023.

[49] V. D. Cong, "Path following and avoiding obstacle for mobile robot under dynamic environments using reinforcement learning," *Journal of Robotics and Control (JRC)*, vol. 4, no. 2, pp. 157-164, 2023.

[50] W. Al-Mayahi and H. Al-Fahaam, "A novel variable stiffness compound extensor-pneumatic artificial muscle (ce-pam): Design and mathematical model," *Journal of Robotics and Control (JRC)*, vol. 4, no. 3, pp. 342-355, 2023.

[51] A. U. Nisa, S. Samo, R. A. Nizamani, A. Irfan, Z. Anjum, and L. Kumar, "Design and Implementation of Force Sensation and Feedback Systems for Telepresence Robotic Arm," *Journal of Robotics and Control (JRC)*, vol. 3, no. 5, pp. 710-715, 2022.

[52] B. L. Widjiantoro, M. K. Wafi, and K. Indriawat, "Non-Linear Estimation using the Weighted Average Consensus-Based Unscented Filtering for Various Vehicles Dynamics towards Autonomous Sensorless Design," *Journal of Robotics and Control (JRC)*, vol. 4, no. 1, pp. 95-107, 2023.

[53] N. S. Abu, W. M. Bukhari, M. H. Adli, S. N. Omar, and S. A. Sohaimeh, "A comprehensive overview of classical and modern route planning algorithms for self-driving mobile robots," *Journal of Robotics and Control (JRC)*, vol. 3, no. 5, pp. 666-678, 2022.

[54] M. Maaruf, A. Babangida, H. A. Almusawi, and P. S. Tamas, "Neural network-based finite-time control of nonlinear systems with unknown dead-zones: Application to quadrotors," *Journal of Robotics and Control (JRC)*, vol. 3, no. 6, pp. 735-742, 2022.

[55] R. Sekhar, P. Shah, and I. Iswanto, "Robotics in industry 4.0: A bibliometric analysis (2011-2022)," *Journal of Robotics and Control (JRC)*, vol. 3, no. 5, pp. 583-613, 2022.

[56] N. E. Fard and R. Selmic, "Consensus of multi-agent reinforcement learning systems: The effect of immediate rewards," *Journal of Robotics and Control (JRC)*, vol. 3, no. 2, pp. 115-127, 2022.

[57] G. Rjoub, J. Bentahar, H. Elmekki, W. Pedrycz, N. Drawel, and S. Kassaymeh, "Deep Reinforcement Learning for Robotics Motion Planning Combining Graph Neural Networks and Multi-Agent Systems," *Available at SSRN 4725188*, 2024.

[58] T. An, J. Lee, M. Bjelonic, F. De Vincenti, and M. Hutter, "Solving multi-entity robotic problems using permutation invariant neural networks," *arXiv preprint arXiv:2402.18345*, 2024.

[59] S. Zhang, A. Guerra, F. Guidi, D. Dardari, and P. M. Djurić, "Multi-Agent Navigation with Reinforcement Learning Enhanced Information Seeking," in *2022 30th European Signal Processing Conference (EUSIPCO)*, pp. 982-986, 2022.

[60] Y. Shaoul, R. Veerapaneni, M. Likhachev, and J. Li, "Unconstraining Multi-Robot Manipulation: Enabling Arbitrary Constraints in ECBS with Bounded Sub-Optimality," in *Proceedings of the International Symposium on Combinatorial Search*, vol. 17, pp. 109-117, 2024.

[61] Z. Salehi, P. Karimaghaee, and M. H. Khooban, "A new passivity preserving model order reduction method: conic positive real balanced truncation method," *IEEE Transactions on Systems, Man, and Cybernetics: Systems*, vol. 52, no. 5, pp. 2945-2953, 2021.

[62] T. Breiten and B. Unger, "Passivity preserving model reduction via spectral factorization," *Automatica*, vol. 142, p. 110368, 2022.

[63] Y. Yun, D. Oh, E. J. Song, H. R. Choi, H. Moon, and J. C. Koo, "Adaptive Passivation of Admittance Controllers by Bypassing Power to Null Space on Redundant Manipulators," in *2024 IEEE/RSJ International Conference on Intelligent Robots and Systems (IROS)*, pp. 9292-9298, 2024.

[64] O. de Groot, L. Valk, and T. Keviczky, "Cooperative passivity-based control of nonlinear mechanical systems," *Robotics*, vol. 12, no. 5, p. 142, 2023.

[65] C. Giamouzis, D. Garyfallou, G. Stamoulis, and N. Evmorfopoulos, "Low-rank balanced truncation of RLCk models via frequency-aware rational Krylov-based projection," in *2024 20th International Conference on Synthesis, Modeling, Analysis and Simulation Methods and Applications to Circuit Design (SMACD)*, pp. 1-4, 2024.

[66] Z. Salehi, P. Karimaghaee, S. Salehi, and M. H. Khooban, "Phase Preserving Balanced Truncation for Order Reduction of Positive Real Systems," *Automation*, vol. 3, no. 1, pp. 84-94, 2022.

[67] A. Y. Lee, W. S. Tsuha, G. K. Man, and G. A. Macala, "Model Reduction Methodologies for Articulated Multi-Flexible Body Systems," in *Structural Dynamic Systems Computational Techniques and Optimization*, pp. 195-271, 2024.

[68] L. Poort, B. Besselink, R. H. Fey, and N. van de Wouw, "Passivity-preserving, balancing-based model reduction for interconnected systems," *IFAC-PapersOnLine*, vol. 56, no. 2, pp. 4240-4245, 2023.

[69] K. Sun, H. Yu, and X. Xia, "Distributed control of nonlinear stochastic multi-agent systems with external disturbance and time-delay via event-triggered strategy," *Neurocomputing*, vol. 452, pp. 275-283, 2021.

[70] L. H. Zhang and R. C. Li, "Quality of Approximate Balanced Truncation," *arXiv preprint arXiv:2406.05665*, 2024.

[71] S. Zhang. *Advanced Distributed Optimization and Control Algorithms: Theory and Applications*. University of North Texas, 2022.

[72] H. Wang, A. Papachristodoulou, and K. Margellos, "Distributed Safety Verification for Multi-Agent Systems," *2023 62nd IEEE Conference on Decision and Control (CDC)*, pp. 5481-5486, 2023.

[73] G. Fedele and G. Franzè, "A distributed model predictive control strategy for constrained multi-agent systems: The uncertain target capturing scenario," *IEEE Transactions on Automation Science and Engineering*, vol. 21, no. 2, pp. 1549-1563, 2023.

[74] S. Guo. *Control and Optimization of Multi-Agent Systems with Applications in Connected and Autonomous Electric Vehicles*. LSU Doctoral Dissertations, 2023.

[75] X. Wang and G. Cheng, "Balanced truncation for discrete time-delay systems via the interpretation of system energy," *Journal of the Franklin Institute*, vol. 359, no. 15, pp. 8243-8264, 2022.

[76] F. J. Mañas-Álvarez, M. Guinaldo, R. Dormido, and S. Dormido, "Robotic park: Multi-agent platform for teaching control and robotics," *IEEE Access*, vol. 11, pp. 34899-34911, 2023.

[77] F. Al-Taie, I. K. Hanan, F. S. Fadhel, and H. S. Abbas, "Coprime Factor Model Reduction of Multidimensional Systems," *Iraqi Journal of Science*, pp. 2186-2197, 2024.

[78] A. Borghi, T. Breiten, and S. Gugercin, "Balanced truncation with conformal maps," *Systems & Control Letters*, vol. 197, p. 106044, 2025.

[79] X. Cheng, J. M. Scherpen, and B. Besselink, "Balanced truncation of networked linear passive systems," *Automatica*, vol. 104, pp. 17-25, 2019.

[80] X. Cheng, J. Scherpen, and H. Trentelman, "Reduced Order Modeling of Large-Scale Network Systems," in *Model Order Reduction*, vol. 3, Feb. 2021.